Theoretical Insights into the Reductive Decompositions of Propylene Carbonate and Vinylene Carbonate: Density Functional Theory Studies

Yixuan Wang* and Perla B. Balbuena*

Department of Chemical Engineering, Swearingen Engineering Center, University of South Carolina, Columbia, South Carolina 29208

Received: November 29, 2001; In Final Form: January 23, 2002

The electroreductive decompositions of propylene carbonate (PC) and vinylene carbonate (VC) in lithium-ion battery-electrolyte solutions have been investigated with density functional theory using $Li^+(PC)_n$ ($n = 2$, 3) and $(PC)_nLi^+(VC)$ ($n = 1$, 2) cluster models. The objective is to help in understanding the experimentally observed irreversible capacity of graphite anodes when PC alone is used as a solvent versus the reported reversible capacity found in the presence of small amounts of VC in PC-based electrolyte solutions. The results indicate that PC solvates Li^+ more strongly than ethylene carbonate (EC) and VC do, which implies that, if it exists, the cointercalation of PC with Li ion into graphite layers is preferred; however, PC is more difficult to be reduced than the other two carbonates. On the other hand, the reaction kinetics for the reductive decomposition of PC is very similar to that of EC. Besides the problem caused by the possible cointercalation, the nature of the PC reduction products may also be responsible for its disability to passivate the graphite surface. The theoretical results suggest the following explanations for the role of VC as an additive: A solvated VC in the $(PC)_nLi^+(VC)$ complex is initially reduced to a more stable ion-pair intermediate, which will undergo a ring-opening reaction by a homolytic C (carbonyl carbon)−O rupture in two ways. One is that the reduced VC decomposes to form a radical anion via a barrier of about 20 kcal/mol and the subsequent radical anion termination would generate the proper products, dominated by unsaturated lithium alkyl dicarbonates, such as lithium vinylene dicarbonate $(CHOCO_2Li)_2$ and lithium divinylene dicarbonate $(CH{=}CHOCO_2Li)_2$, to build up an effective solid electrolyte interfacial (SEI) film. The unsaturated lithium dicarbonates may be further polymerized, forming lithium polyvinylene dicarbonate or oligomers with several repeated CH=CH units that would considerably improve the passivation of graphite electrode in the presence of VC because of formation of a more cohesive and flexible film. The alternative way is that, starting from the VC-reduction intermediate, a ring opening occurs on the unreduced PC moiety rather than on the reduced VC, via a lower barrier. Briefly, VC plays an important role in terms of thermodynamic factors by somehow weakening the PC cointercalation into graphite, stabilizing the reduction ion-pair intermediate, and generating more proper film-forming agents.

1. Introduction

Lithium-ion batteries are becoming popular power sources for advanced portable electronics such as notebook computers and cellular phones because they could provide a good combination of high-energy density and reversibility;[1] the relevant chemistry problems thereby are attracting much attention both from experimentalists and from theoreticians. A typical lithium-ion battery system is made up of a graphitic carbon anode, a nonaqueous organic electrolyte that acts as an ionic path between electrodes and separates the two electrode materials, and a transition-metal oxide (such as$LiCoO_2$, $LiMn_2O_4$, and $LiNiO_2$) cathode. The most usual electrolytes are mixtures of alkyl carbonates, for example, ethylene carbonate (EC), propylene carbonate (PC), and lithium salts such as $LiAsF_6$ and $LiPF_6$. It is generally recognized that organic electrolytes are decomposed during the first lithium intercalation into graphite to form a solid electrolyte interfacial (SEI) film between the graphite anode surface and the electrolyte; this film is a determinant factor on the performance of graphite as anode in rechargeable batteries.[2]

The reductive decomposition of EC, a less useful solvent at room temperature because of its high melting point of 37 °C, has turned out to result in products that build up a stable SEI.[3] Thereby, EC-based solvent mixtures containing a large amount of linear carbonates such as dimethyl carbonate (DMC) are widely used in lithium-ion batteries.[4,5] To determine the SEI composition and its buildup mechanism, a wide variety of advanced experimental techniques have been used.[3,6] In our previous paper, quantum chemistry calculations have also been carried out to get insights on the elementary electro-decompositions of EC in the presence of Li^+ and bulk solvent.[7] It was demonstrated that electrons would be initially transferred from the polarized electrode to the Li^+ coordinated EC molecules, forming ion-pair intermediates. Then, a homolytic ring opening will take place on the intermediates to generate radical anions, which will participate in termination reactions resulting in proper products in the form of Li organic and inorganic salts, building up the SEI film, which may even penetrate into the graphite structure.[8] In line with some experimental findings, two-electron reduction processes indeed take place by stepwise paths to generate the inorganic Li_2CO_3,[4] and the Li carbides containing Li−C bonds,[5,9] respectively. Regarding the solvent reduction products, it was found that they are comprised by two leading lithium alkyl dicarbonates,$(CH_2CH_2OCO_2Li)_2$ and $(CH_2OCO_2Li)_2$, together with $LiO(CH_2)_2CO_2(CH_2)_2OCO_2Li$ and a small

* E-mails: wangyi@engr.sc.edu and balbuena@engr.sc.edu.

10.1021/jp014371t CCC: $22.00
Published on Web 04/02/2002

amount of $Li(CH_2)_2OCO_2Li$ and Li_2CO_3.[7] Among them, besides the identification of the last two species as SEI components, experimentalists commonly consider $(CH_2OCO_2Li)_2$ as a dominant component of SEI on either the Li or Li−C electrode surface, and the possibility of $(CH_2CH_2OCO_2Li)_2$ as a SEI species is also suggested in EC-based solution (EC-DMC−$LiAsF_6$, highly oriented pyrolytic graphite) by Bar-Tow et al.[9] as well as by Naji et al. (EC−$LiClO_4$, natural graphite),[10] whereas so far $LiO(CH_2)_2CO_2(CH_2)_2OCO_2Li$ has never been experimentally identified as a SEI component.

PC is an attractive solvent for nonaqueous electrolyte batteries because of its superior ionic conductivity over a wide temperature range. However, despite the close structural similarity between EC and PC, PC behaves completely different, that is, the graphite electrode is destroyed and no effective SEI is formed on the graphite surface when pure PC alone is used as a solvent.[11] Regarding the stable SEI film formation in EC solution and the destructive reaction behavior in PC, the explanations from different groups are still controversial. Besenhard et al. suggested that the solvent can cointercalate into the graphite layer structure to form a ternary graphite intercalation compound (GIC) $[Li(sol)_yC_n]$,[8,11,12] the decomposition products of EC forming a stable SEI film[8,12] whereas those of PC exert an intense stress on the graphite electrode such that its structure is destroyed.[11,12] Very recently, using in situ atomic force microscopic (AFM) observations were done on the basal plane of highly oriented pyrolytic graphite (HOPG, in LiClO4−EC−DEC) by Ogumi et al.[13] These researchers found that atomically flat areas of 1- or 2-nm height (hill-like structures) and large swellings of 15−20-nm height (blisters) appeared on the surface. They suggested that the two features were caused by the intercalation of EC-solvated lithium ions and their decomposition beneath the surface, respectively. Another model, originally proposed by Peled et al.[14,15] and further developed by Aurbach et al.,[4] raises concerns on the existence of solvent cointercalation, stressing that PC is reduced even before its cointercalation; thus, it is the disability of its reduction products to form an effective SEI film which leads to the destruction of the graphite electrode. However, Chung et al.[16] went back to the explanation that the cointercalation of PC provides a more adequate explanation of the change in the graphite structure than a simple surface reduction of PC after a comprehensive study using EC, PC, and cis and trans 2,3-butylene carbonate electrolyte solutions, respectively.

Many efforts have been dedicated to find proper additives to PC-based electrolytes, which would help to generate an efficient SEI layer. Some successes have been reported, including the addition of chloroethylene carbonate (CEC), other halogen-substituted carbonates,[17] and a variety of unsaturated carbonates such as vinylpropylene carbonate,[18] vinylene carbonate (VC), and ethylene sulfite (ES).[19] Often present in small amounts (5∼10% volume), these additives, together with solvents (PC, or mixtures of EC and PC), could form the desirable protective interfaces, that is, a protective SEI layer. However, there are very few reported studies about the mechanism by which these additives act efficiently increasing the performance of lithium-ion batteries, and the choice of such kind of additives depends on costly trial-and-error experiments. To design an additive on a rational basis, such that the reaction behavior of PC could be prohibited or suppressed, it is quite necessary to understand the reaction mechanism of PC taking place in lithium-ion battery electrolytes and to identify the mechanisms by which the additives would considerably modify the buildup of the SEI film in the PC-based electrolytes.

In the present article, the reductive decomposition mechanisms of PC are first investigated using $Li^+(PC)_2$ and $Li^+(PC)_3$ supermolecular cluster models, then the effect of VC on them is analyzed with the $(PC)Li^+(VC)$ and $(PC)_2Li^+(VC)$ models. On the basis of these calculated results coupled with the previous studies of EC reduction, the reasons for the PC failure and for the VC efficient role as an additive are discussed at the molecular-scale level.

2. Computational Details

All the calculations have been performed using the Gaussian 98 program.[20] The equilibrium and transition state structures are fully optimized by the B3PW91 method[21−24] using 6-31G(d) basis set, and frequency analyses are done with the same basis sets to confirm the transition states and to obtain zero-point energy (ZPE) corrections. The single-point energies for the B3PW91/6-31G(d)-optimized geometries are calculated at the B3PW91/6-311++g(d,p) level. If not noted otherwise, relative energies refer to those with ZPE correction, and enthalpies and Gibbs free energies are calculated at 298.2K. Charges are calculated by fitting the molecular electrostatic potential (CHELPG method).[25]

Several strategies are used to investigate the role of solvent effects. In a first stage, specific solvent molecules are explicitly included in the calculations with the molecular clusters $(PC)_nLi^+$ ($n = 2, 3$) and $(PC)_nLi^+(VC)$ ($n = 1, 2$) in gas phase. Since the conductor-like polarizable continuum model (CPCM)[26] could give much more consistent errors on nuclear and electronic total polarization as compared with the dielectric PCM, the bulk solvent effects are then estimated for $(PC)_2Li^+$ and $(PC)Li^+$-(VC) at the CPCM-B3PW91/6-311++G(d,p)//B3PW91/6-31G-(d) level. Despite the fact that this method provides less reliable absolute values of solvent energies, it is adequate for the evaluation of relative values between closely related species. In the CPCM model, the variation of the free energy when going from vacuum to solution is composed of the work required to build a cavity in the solvent (cavitation energy) together with the electrostatic and nonelectrostatic work (dispersion and repulsion energy),[27] whose sum is referred to as W_0. A conventional set of Pauling radii and tetrahedral cavity with 64 initial tesserae has been used for all CPCM calculations. In the present article, we term the above treatment, consisting of a continuum model calculation (optimization or single-point calculation) based on the fully optimized clusters in the gas phase, as cluster-continuum model.

To gain insights into the bonding characteristics between Li and solvent molecules, we have also applied the atoms in molecules (AIM) theory of Bader[28] to some of the species. AIM is based on a topological analysis of electron density function $\rho(r)$ and of its Laplacian $\nabla^2\rho(r)$ at the bond critical point (bcp). It is well established that the interactions between closed-shell systems (ionic bond, hydrogen bond, van der Waals molecules, etc.) demonstrate $\nabla^2\rho(r) > 0$, while the inverse $\nabla^2\rho(r) < 0$ corresponds to covalent bonds.

3. Results and Discussion

3.1 Solvation of Li^+ in Organic Electrolyte Solutions. Carbonate molecules strongly solvate Li^+ in organic nonaqueous electrolytes of Li-ion battery, and such solvation also considerably affects the solvent reduction potentials and the subsequent decomposition reactions, for example, the solvent molecules coordinated to lithium ions would be prone to react with the electrode.[7] For these reasons, the solvation of lithium ions in the electrolyte solutions of lithium-ion batteries is an interesting

TABLE 1: The $Li^{+-}O$ Distances (r/Å), ZPE-corrected Average Binding Energies between Li^+ and PC (BE, kcal/mol), Heats of Reaction (ΔH_r, kcal/mol), and Gibbs Free Energies of Reaction (ΔG_r, kcal/mol) at 298.2 K Calculated by B3PW91/6-31G(d)

reactions	r[a]	BE'[b]	BE	ΔH_r'[c]	ΔG_r'	ΔH_r	ΔG_r
1. Li^++PC→Li^+(PC)	1.760	51.9	49.5	−52.1	−46.0	−49.7	−43.6
	(1.746)	(49.6)	(49.1)	(−50.0)	(−43.2)	(−49.5)	(−42.7)
2. $Li^+(PC)$+PC→$Li^+(PC)_2$	1.811	45.8	42.9	−39.2	−31.9	−36.0	−28.7
3. $Li^+(PC)_2$+PC→$Li^+(PC)_3$	1.893	38.6	35.6	−23.5	−14.6	−20.1	−11.2
4. $Li^+(PC)_3$+PC→$Li^+(PC)_4$	1.968	32.7		−15.3	−1.6	−11.7	+2.0
5. Li^++EC→Li^+(EC)[d]	1.764	50.3	46.4	−50.6	−45.0	−47.7	−42.1
	(1.742)	(48.0)	(47.4)	(−48.4)	(−42.1)	(−47.8)	(−41.5)
6. Li^+(EC)+EC→$Li^+(EC)_2$	1.814	44.7	40.6	−38.5	−30.8	−35.3	−27.6
7. $Li^+(EC)_2$+EC→$Li^+(EC)_3$	1.893	37.8	33.9	−24.2	−12.7	−20.9	−9.4
8. $Li^+(EC)_3$+EC→$Li^+(EC)_4$	1.965	33.2		−13.9	−5.9	−10.4	−2.4
9. Li^++VC→ Li^+(VC)	1.772	46.4	44.8	−46.9	−40.5	−44.3	−37.9
	(1.759)	(44.0)	(43.4)	(−44.5)	(−37.5)	(−43.9)	(−36.9)
10. Li^+(PC)+VC→(PC)Li^+(VC)	1.808/1.826	43.6	40.8	−34.8	−27.6	−31.8	−24.6
11. $Li^+(PC)_2$+VC→(PC)Li^+(VC)+PC				4.4	4.3		
12. $Li^+(PC)_2$+VC→$(PC)_2Li^+$(VC)				−20.4	−12.0		
13. $Li^+(PC)_3$+VC→$(PC)_2Li^+$(VC)+PC				3.1	2.6		

[a] Average bond lengths from Li^+ to the carbonyl oxygen; the data in parentheses from B3PW91/6-311++G(d,p). [b] The symbols with prime refer to without BSSE correction; $BE = -\{E[Li^+(PC)_n] - nE[(PC)] - E(Li^+) + ZPE + BSSE\}/n$. [c] $\Delta H_r = H[Li^+(PC)_n] - H[Li^+(PC)_{n-1}] - H(PC)$, the same definition for ΔG_r . [d] The data for $Li^+(EC)_n$ without BSSE from ref 7.

TABLE 2: Relative Energies, Enthalpies, and Free Energies (in kcal/mol), Charge (*q*/e), Main Coefficients of Spin Densities (sd/e) for Stationary Points, and Imaginary Frequency (ω/cm^{-1}) for Transition States in $Li^+(PC)_2$ and $Li^+(PC)_3$

						q[f]		sd[g]			
structures	ΔE[a]	$\Delta E(0)$[b]	ΔE_0[c]	ΔH[d]	ΔG[e]	Li	CO_3	C1	Li	C2	w
$Li^+(PC)_2$											
1	0.0	0.0	0.0	0.0	0.0	+0.93	−0.58				
2	**−65.4**	−67.3	−69.3	−69.6	−68.0	+0.78	−1.22	0.67			
3(TS,2↔4)	**−50.9**	−54.7	−57.8	−57.9	−56.4	+0.72	−1.16	0.44		0.40	−910
4	**−90.6**	−94.2	−98.3	−97.7	−99.0	+0.70	−1.00			1.00	
5	**−55.0**	−56.2	−58.6	−58.5	−57.5	−0.30	−0.48		0.92		
$Li^+(PC)_3$											
6	0.0	0.0	0.0	0.0	0.0	+0.84	−0.53				
7	**−56.1**	−57.8	−61.8	−62.1	−57.7	+0.65	−0.87	0.70			
8 (TS,7↔9)	**−42.1**	−46.1	−50.0	−50.2	−45.2	+0.69	−1.12	0.46		0.40	−910
9	**−80.5**	−84.0	−88.5	−88.0	−86.2	+0.72	−1.03			1.04	

[a] ΔE(B3PW91/6-31G(d)). [b] $\Delta E(0)$: ΔE(B3PW91/6-31G(d))+ ΔZPE(B3PW91/6-31G(d)). [c] ΔE_0: ΔE(B3PW91/6-311++G(d,p)//B3PW91/6-31G(d))+ ΔZPE(B3PW91/6-31G(d)). [d] ΔH: ΔE(B3PW91/6-311++G(d,p)//B3PW91/6-31G(d))+$\Delta\Delta H$(B3PW91/6-31G(d)). [e] ΔG: ΔE (B3PW91/6-311++G(d,p)//B3PW91/6-31G(d))+ $\Delta\Delta G$(B3PW91/6-31G(d). [f] CO_3 group belongs to the reactive PC molecule. [g] C1 and C2 refer to carbonyl carbon and ethereal carbon, respectively.

and still a controversial topic.[29,30] The supermolecules $Li^+(PC)_n$ ($n = 1\sim4$) were fully optimized by B3PW91/6-31G(d) method. For $Li^+(PC)_2$, two nearly degenerate structures were located. One is a pseudo-planar structure, whereas in the other, two PC ligands are perpendicular to each other. For $Li^+(PC)_3$, the PC molecules are trigonal planar, and pseudo-tetrahedral for Li^+-$(PC)_4$. Table 1 summarizes the binding characteristics for these supermolecules, that is, the average bond distances (*r*) from the lithium cation to the carbonyl oxygen, binding energy per solvent (BE), the heats of formation, and Gibbs free energies of formation. The basis set superposition error (BSSE)-corrected energetic data for the two types of basis set agree within 1.0 kcal/mol. *r* increases with the number of PC molecules, and BE monotonically decreases. The positive BSSE-corrected ΔG_r of $Li^+(PC)_4$ indicates that the formation of $Li^+(PC)_4$ is not favorable; this conclusion is in line with a recent electrospray ionization mass spectroscopy (ESI-MS) study[30] in which a four-coordinated Li^+ species was not found, instead $Li^+(PC)_2$ and $Li^+(PC)_3$ are the two major solvated lithium ion species, with the concentration of $Li^+(PC)_3$ being higher than that of Li^+-$(PC)_2$.

The BEs of $Li^+(PC)_n$ are higher by approximately 2.0 kcal/mol than those of $Li^+(EC)_n$, and their corresponding ΔG_r are about 1.5 kcal/mol more negative except for the four-coordinated cases for which the ΔG_r of $Li^+(PC)_4$ is 4.4 kcal/mol more positive than that of $Li^+(EC)_4$ (+2.0 vs −2.4 kcal/mol). The weak binding character between Li^+ and PC or Li^+ and EC is revealed by the positive $\nabla^2\rho(r)$ obtained by AIM calculations at B3PW91/6-311++G (d,p) for Li^+(S) systems: $\rho(r) = 0.043$ au, $\nabla^2\rho(r) = 0.379$ at the bcp between Li^+ and the PC carbonyl oxygen, and $\rho(r) = 0.042$ au, and $\nabla^2\rho(r) = 0.372$ at the bcp between Li^+ and the EC carbonyl oxygen. The present results support the speculation of Chung et al. that PC solvates Li^+ more strongly than EC,[31] and they also agree with the findings of Fukushima et al. that the lithium ion is solvated preferentially by PC in a $LiClO_4$/EC−PC−MeOH (0.5:1.0:9.0 volume) solution.[30] However, they are completely different from those of Klassen et al.,[29] who obtained higher solvation energies for EC to Li^+ than for PC at the HF/6-311++G(d,p) level and also concluded that EC selectively solvates Li^+ in the EC/PC/$LiClO_4$ binary solvent solution on the basis of the analyses of conductivity and viscosity measurements.

3.2 Reductive Decompositions of $Li^+(PC)_2$ and of Li^+-$(PC)_3$. The relative energetic data are summarized in Table 2, together with electronic characteristics for the species of interest on the $Li^+(PC)_2$ (**1**) and $Li^+(PC)_3$ (**6**) reductive decomposition paths. The corresponding energy surfaces of $Li^+(PC)_2$ and Li^+-$(PC)_3$ are illustrated in Figures 1 and 2, respectively, in which those of $Li^+(EC)_2$ and $Li^+(EC)_3$[7] are also included for comparison. As in of $Li^+(EC)_2$, an ion-pair intermediate **2** (Figure 1) is found for $Li^+(PC)_2$, in which the unpaired spin density is mainly located at the carbonyl carbon (C1) with a coefficient

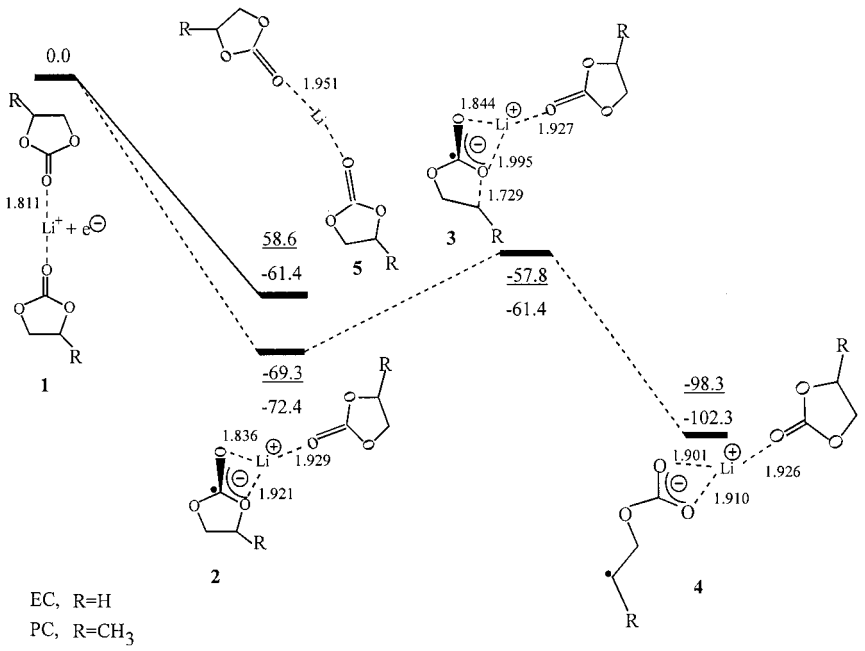

Figure 1. Potential energy profile for the reductive decomposition process of $Li^+(PC)_2$ (underlined data) and $Li^+(EC)_2$ (plain data)[7] calculated with B3PW91/6-311++G(d,p)// B3PW91/6-31G(d). The selected structural data refer to the $Li^+(PC)_2$ species.

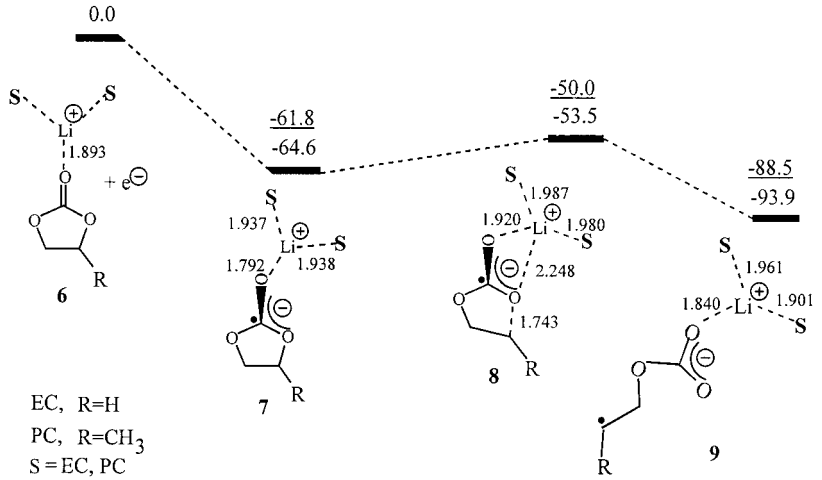

Figure 2. Potential energy profile for the reductive decomposition process of $Li^+(PC)_3$ (underlined data) and $Li^+(EC)_3$ (plain data)[7] calculated with B3PW91/6-311++G(d,p)// B3PW91/6-31G(d). The selected structural data refer to the $Li^+(PC)_3$ species.

of 0.67. The reduction intermediate could undergo a homolytic ring opening by the cleavage of C−O bond via the transition state (TS) **3**, resulting in a radical anion coordinated with Li^+, **4**. In line with the energy levels of the lowest unoccupied molecular orbitals (LUMO, −0.1173 vs −0.1230 au), where the main components come from the carbonyl carbon of $Li^+(PC)_2$ and $Li^+(EC)_2$, Figure 1 shows that the adiabatic electron affinity (EA, $\sim \Delta E_0$) of $Li^+(PC)_2$ is 3.1 kcal/mol lower than that of $Li^+(EC)_2$ (69.3 vs 72.4 kcal/mol). The formation energy of the radical anion **4** (referred to as E_f hereafter, relative to $Li^+(PC)_2$) is also somewhat lower than that of $Li^+(EC)_2$ (98.3 vs 102.3 kcal/mol); however, the ring-opening energy barrier (E_a) of **2** is basically identical with that of the intermediate of $Li^+(EC)_2$ (11.5 vs 11.0 kcal/mol). The species **5** is the other reduction intermediate in which the reduction occurs on the Li, consequently bearing the dominant spin density with a coefficient of 0.92 e.

Compared with $Li^+(PC)_2$, the adiabatic EA of $Li^+(PC)_3$ is further reduced by approximately 7.5 kcal/mol, so is E_f of the radical anion. However, the energy barrier for ring opening of the radical anion changes negligibly (11.8 vs 11.5 kcal/mol). This shows that the values of EA and E_f of $Li^+(PC)_n$ are considerably influenced by the solvent, while the solvent effect on E_a is rather weak. Additionally, although the ring-opening barrier E_a is again close (11.8 vs 11.1 kcal/mol), EA and E_f of $Li^+(PC)_3$ are lower than those of $Li^+(EC)_3$ by 2.8 and 5.4 kcal/mol, respectively. The bulk solvent effect, incorporated by CPCM using the gas-phase optimized geometries, further remarkably decreases the EA of $Li^+(PC)_2$ from 69.3 kcal/mol in the gas phase to 44.4 kcal/mol ($W_0 = -40.7$ and -14.6 kcal/mol for **1** and **2**, respectively), and it slightly reduces E_a by 2.1 kcal/mol ($W_0 = -16.7$ kcal/mol for TS **3**). The reduction potential predicted by the cluster-CPCM method for the red-ox reaction ($\Delta G_{sol} = \Delta G$ in the gas phase $+ \Delta W_0$)

$$(PC)_2\cdots Li^+ (\mathbf{1}) + e^- \rightarrow [(PC)^{\bullet -}]\cdot\cdot Li^+\cdots(PC)\ (\mathbf{2}), \quad (I)$$

is 1.82 V, and it is 0.14 V lower than that of $Li^+(EC)_2$ (1.96

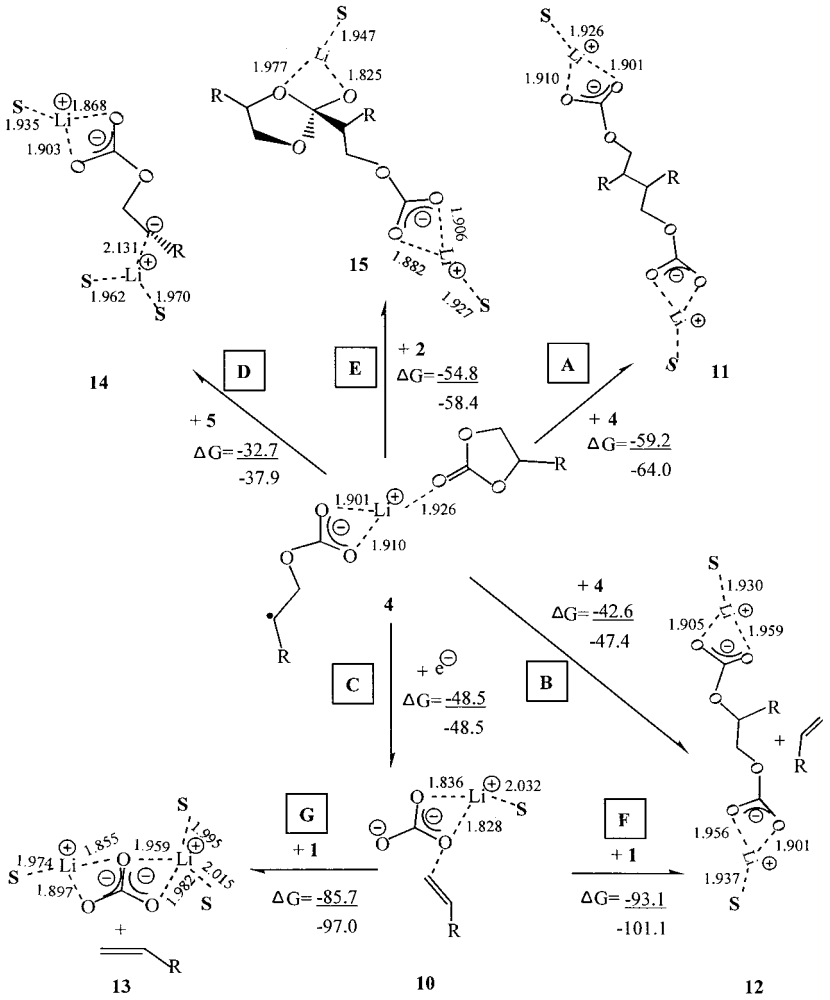

Figure 3. The termination paths for the radical anion from the reductive dissociation in $Li^+(PC)_2$ calculated with B3PW91/6-311++G(d,p)//B3PW91/6-31G(d) method. ΔG_r at 298.15 K of the underlined and plain data refer to $Li^+(PC)_2$ (S = PC, R = CH_3) and $Li^+(EC)_2$ (S = EC, R = H),[7] respectively. The selected structural data refer to the $Li^+(PC)_2$ reduction species.

V[7]). On the basis of the DFT results, a comparison between $Li^+(PC)_n$ and $Li^+(EC)_n$ (n = 2 and 3) indicates that although the initial electro-reductions of EC and PC are qualitatively similar on the kinetic aspects, such as the reduction mechanism as well as the ring-opening energy barrier, the quantitative difference on the thermodynamics is worth to be noticed, for example, the reduction potential of PC calculated by the cluster-CPCM model is approximately 0.1 ∼ 0.2 V lower than that of EC, and the formation of radical anion releases less energy. Coupled with the aforementioned stronger binding of PC with Li^+, our preliminary impression about the difference between PC and EC properties as Li-ion battery solvents is that the cointercalation, if it exists, of PC with Li^+ into the graphite layers is favored; however, the PC reduction potential is lower than EC. Whether these factors partially lead to their complete different behaviors or not needs to be further investigated.

3.3 Termination Reactions of the Radical Anion. The possible termination reactions of the radical anion **4** have been examined (shown in Figure 3, along with specific data reported in Table 3) to evaluate whether the nature of the products should be responsible for the PC failure to form an effective SEI film. It is expected that the barrierless combination (path **A**) via the radical center to form solvated lithium di-isopropyl carbonate[32] (2,3-dimethyllithium butylene dicarbonate), $(CH_3CHCH_2OCO_2Li)_2$, **11**, would be the most possible reaction. The Gibbs free energy of reaction for path **A** (ΔG = −59.2 kcal/mol) indeed is the most favorable among the involved reactions. Aurbach et al.[32] suggested the possibility of **11** as a SEI species on lithium surfaces from the fact that the percentage of the alkyl carbon XPS peak around 285−286 eV is much higher than that expected from the product **12** alone, whereas the corresponding compound, lithium butylene dicarbonate $(CH_2CH_2OCO_2Li)_2$, for EC-based electrolyte was also proposed on the graphitic carbon surface by Naji et al.[9,10] Nevertheless, we still need more

TABLE 3: Relative Energies, Enthalpies, Free Energies (in kcal/mol), and Charges (q/e) in the Potential Energy Surface of $Li^+(PC)_2$

						q[f]	
structures	ΔE[a]	$\Delta E(0)$[b]	ΔE_0[c]	ΔH[d]	ΔG[e]	Li	CO_3
1	0.0	0.0	0.0	0.0	0.0	+0.93	−0.58
10	**−131.2**	−135.7	−149.7	−149.3	−147.5	+0.73	−1.58
11/2	**−130.7**	−131.1	−134.2	−134.1	−127.0		
12/2	**−123.2**	−124.9	−128.9	−128.3	−122.0		
13/2	**−124.9**	−126.5	−128.5	−128.3	−119.7		
14/2	**−99.3**	−100.6	−102.6	−102.4	−94.6		
15/2	**−117.0**	−117.1	−118.1	−118.6	−107.8		

[a] ΔE(B3PW91/6-31G(d)). [b] $\Delta E(0)$: ΔE(B3PW91/6-31G(d))+ ΔZPE-(B3PW91/6-31G(d)). [c] ΔE_0: ΔE(B3PW91/6-311++G(d,p)//B3PW91/6-31G(d))+ΔZPE(B3PW91/6-31G(d)). [d] ΔH: ΔE(B3PW91/6-311++G-(d,p)//B3PW91/6-31G(d))+$\Delta\Delta H$(B3PW91/6-31G(d)). [e] ΔG: ΔE(B3PW91/6-311++G(d,p)//B3PW91/6-31G(d))+ $\Delta\Delta G$(B3PW91/6-31G(d). [f] CO_3 group belongs to the reactive PC molecule.

evidences to identify **11** and lithium butylene dicarbonate as SEI film components in PC and EC-based electrolyte, respectively. Nucleophilicly attacking the radical center by oxygen, the radical anion **4** could undergo another dimerization (the corresponding transition state has not been found, path **B**), generating propylene gas and an insoluble compound in polar organic electrolyte, lithium propylene dicarbonate, $CH_3CH(OCO_2Li)CH_2(OCO_2Li)$, **12**, which has commonly been identified as a major SEI component on the Li surface;[32] its chemical analogue, $(CH_2OCO_2Li)_2$, is also one of the most common products identified experimentally from the EC reductive decomposition.[5,6,9,10,32] The third termination pathway is the further reduction by another electron transfer transferred from the polarized electrode (path **C,** $\Delta G = -48.5$ kcal/mol), by which a weak complex **10** of propylene gas and an unpaired nucleophilic carbonate anion ($LiCO_3^-$) are generated. The carbonate anion ($LiCO_3^-$) may either precipitate as insoluble inorganic lithium carbonate Li_2CO_3, **13**, by ion pairing with the solvated Li ion of $Li^+(PC)_2$ (path **G**, $\Delta G = -85.7$ kcal/mol), or it can nucleophilicly attack a solvent molecule of $Li^+(PC)_2$ to form lithium propylene dicarbonate **12** (path **F**, $\Delta G = -93.1$ kcal/mol).

Additionally, the radical anion could also react with the intermediates **2** and **5**. One pathway leads to the possibility to form a species with C−Li bond (Li carbides), **14**, $CH_3Li(CH)(CH_2)OCO_2Li$, via the reaction with **5** (path **D**, $\Delta G = -32.7$ kcal/mol). The corresponding path has been discovered for EC reductive decomposition in Li-ion battery with the XPS technique.[5,9] According to the usual definition, the formation of the Li carbide species proceeds via a two-electron reduction mechanism like that of path **C**, and the difference is merely that the added electrons are distributed on the two separate species (**4** and **5**) instead of being added in a continuous process to one species such as **10**. Another possible way is the combination of **4** with the other reduction intermediate **2** (path **E**, $\Delta G = -54.8$ kcal/mol) that generates an organic lithium salt, $LiOCH_3CHCH_2CO_2CHCH_3CH_2OCO_2Li$, **15**. However, **15** and its chemical analogue, $LiO(CH_2)_2CO_2(CH_2)_2OCO_2Li$, so far have not been experimentally identified as SEI species.

Comparing the Gibbs free energies of reaction (ΔG) for the involved radical terminations of $Li^+(EC)_2$ cluster, path **C** has virtually identical value with the corresponding path in $Li^+(EC)_2$, whereas the other paths generally have less negative ΔG. As shown in Figure 3, the ΔG's of paths **A**, **B**, **D**, and **E** are 4.8, 4.8, 5.2, and 3.6 kcal/mol less negative than those corresponding to $Li^+(EC)_2$. For paths **F** and **G**, they are much less negative by 8.0 and 11.3 kcal/mol than those of $Li^+(EC)_2$, and path **F** has a negative ΔG higher by 7.4 kcal/mol than path **G**. Consequently, path **F** generating lithium propylene dicarbonate is much more favorable than path **G** leading to the inorganic product, Li_2CO_3, in PC than in EC (−93.1 vs −85.7 kcal/mol in PC, −101.1 vs −97.0 kcal/mol in EC). The inorganic compound, lithium carbonate, is usually considered as a better passivating agent than the organic one; however, from the analysis of solvent reduction it can be concluded that Li_2CO_3 plays a minor role in the SEI buildup even in EC-based electrolyte, and the present results indicate that such possibility becomes even lower in a PC-based solvent. Besides this difference, the other product distribution is very similar to that found in EC, for example, the lithium alkyl dicarbonate with long chain constitutes the most important component, followed by R−O−Li and another lithium alkyl dicarbonate with short chain, and the least the C−Li carbide compound. Therefore, at this stage it is not so convincible whether the destructive behavior of PC toward graphite is due to the nature of the solvent decomposition products as well. Perhaps the mechanical performance such as product adhesion ability is the most important reason,[33] that is under investigation by MD and other techniques.

3.4 The Reductive Decomposition of VC and PC in (PC)-Li^+(VC) and $(PC)_2Li^+$(VC) Clusters. To realistically represent the addition of a small amount of VC into the PC-based electrolyte solution, the formation of clusters $(PC)Li^+(VC)$ (**16**) and $(PC)_2Li^+(VC)$ (**24**) are estimated by the reactions 10−13 shown in Table 1. Thermodynamic data without inclusion of solvent effect indicate that they could be generated through the addition reactions 10 and 12, rather than by the substitution reactions 11 and 13. Their reduction paths are shown in Figure 4 and Figure 5, respectively, and their energetic data are listed in Table 4. Figure 4 illustrates the ion-pair reduction intermediates, **17** and **18**, which correspond to the reductions of VC and PC, respectively. VC reduction generates a more stable intermediate than PC reduction by approximately 5 kcal/mol, which shows that VC has about 0.2∼0.3 eV higher electron affinity than PC. The energy barrier of the C−O bond homolytic cleavage in the VC moiety of **17** via TS **19** is 20.1 kcal/mol, which is rather close to that of $Li^+(VC)$ (20.6 kcal/mol) as well as the corresponding barrier of $(EC)Li^+(VC)$ (20.4 kcal/mol).[34]

Because of a stronger solvent effect (dielectric constants of VC and PC: 127[35] and 66.14, respectively, at room temperature) compared with **2** of $Li^+(PC)_2$, the PC-reduction intermediate **18** gets 2.7 kcal/mol higher stabilization energy (the relative energies −72.0 vs −69.3 kcal/mol), and the radical anion **22** is also more stable by about 3.1 kcal/mol. However, the homolytic ring-opening barrier of the PC-reduction intermediate via TS **21** actually remains the same as that of **2** (11.5 kcal/mol). Although **18** has 4.8 kcal/mol higher energy than **17** in gas phase, the ring opening of the former results in a more stable radical anion (**22**) than the latter (**20**) by 10.2 kcal/mol. As shown on the potential energy surface of Figure 4, the ring-opening TS **23** of the PC moiety in the intermediate **17** is also located, in which the unpaired spin density is located at the carbonyl carbon of VC with a coefficient of 0.44, at the leaving ethereal carbon of PC with 0.30 and at the lithium atom with 0.15 (not shown in Table 4). The characteristics of **23** as a transition state connecting **17** and the more stable intermediate **22** have been confirmed by the vibrational modes of its eigenvectors as well as by IRC calculations. The energy barrier of **17** via TS **23** is only 14.8 kcal/mol, which is 5.3 kcal/mol lower than the opening of VC via TS **19** and only 3.3 kcal/mol higher than the homolytic ring opening of **18** via TS **21**. Taking into account thermodynamic as well as kinetic aspects of the ring opening for the supermolecule $(PC)Li^+(VC)$, it is concluded that the optimal reductive decomposition path of $(PC)Li^+(VC)$ starts with the initial reduction of VC to the more stable ion-pair intermediate **17**. **17** will undergo a homolytic ring opening on PC instead of on the reduced VC via an intramolecular electron-transfer TS **23,** to avoid overcoming a high-energy barrier, generating the more stable radical anion **22**. For this decomposition process, VC is not consumed; it just catalyzes the homolytic ring opening of PC via the formation of a stable ion-pair intermediate. Bulk solvent effects on the reduction potentials and ring-opening barriers of the ion-pair intermediates have also been estimated by the CPCM method (dielectric constant ϵ, 66.14). The cluster-CPCM predicted ring-opening barriers for TS **19**, **21**, and **23** are only decreased by 1.0, 0.6, and 2.2 kcal/mol, respectively (Figure 4). The reduction potentials also estimated by the CPCM-cluster method for the

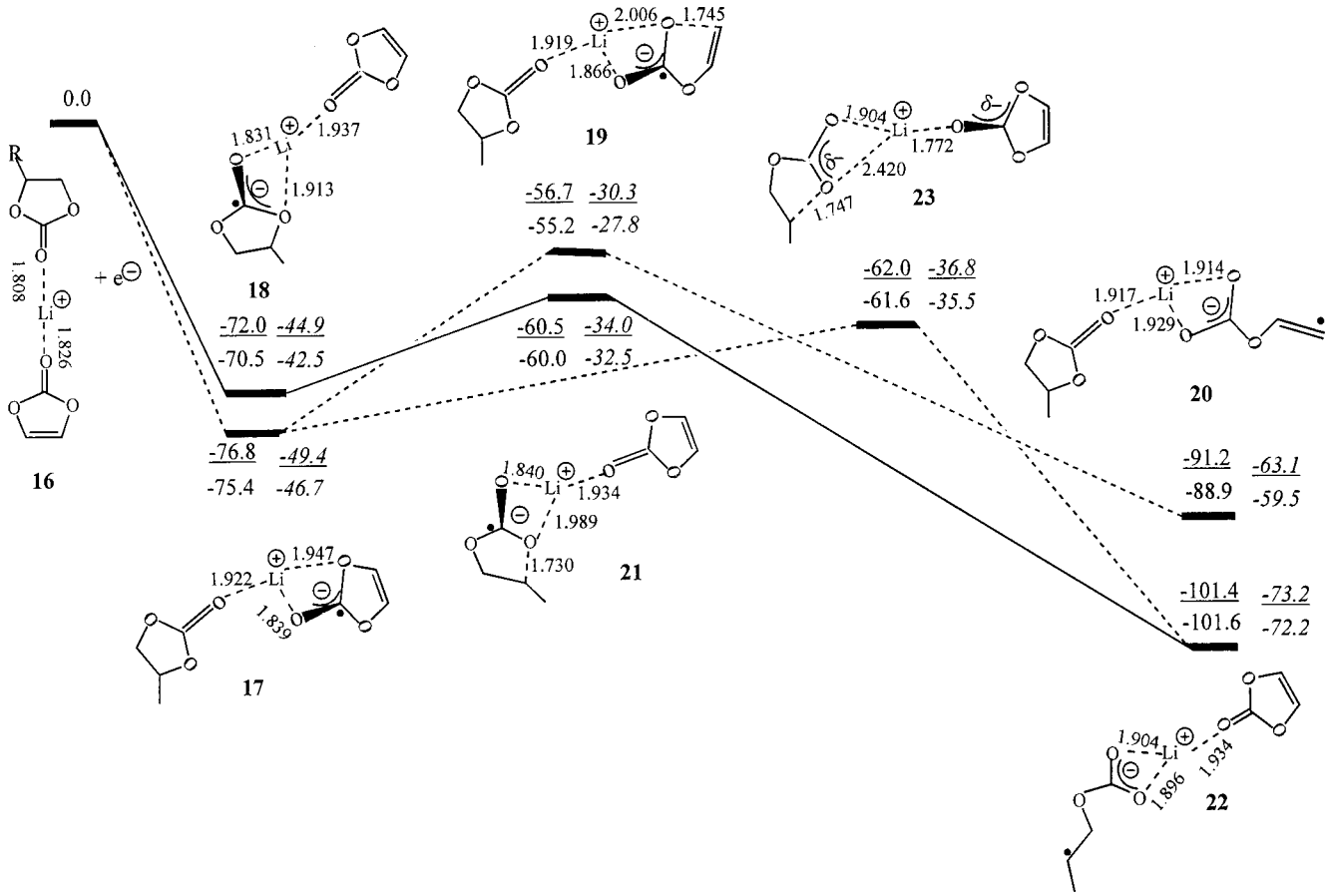

Figure 4. The potential energy (underlined data) and Gibbs free energy profile at 298.15 K for the reductive decomposition process of $(PC)Li^+$-(VC) with the B3PW91/6-311++G(d,p)//B3PW91/6-31G(d) method. The italic data refer to the results from $(PC)Li^+(VC)$-CPCM-B3PW91/6-311++G(d,p)//B3PW91/6-31G(d).

following red-ox reactions:

$$(PC)\cdots Li^+\cdots(VC)\,(\mathbf{16}) + e^- \rightarrow (PC)\cdots Li^+\cdot\cdot[(VC)^{\bullet -}]\,(\mathbf{17}), \quad \text{(II)}$$

$$(PC)\cdots Li^+\cdots(VC)\,(\mathbf{16}) + e^- \rightarrow (PC)\cdots Li^+\cdot\cdot(CO_3)^-CH{=}\,^{\bullet}CH\,(\mathbf{20}), \quad \text{(III)}$$

$$(PC)\cdots Li^+\cdots(VC)\,(\mathbf{16}) + e^- \rightarrow [(PC)^{\bullet -}]\cdot\cdot Li^+\cdots(VC)\,(\mathbf{18}), \quad \text{(IV)}$$

$$(PC)\cdots Li^+\cdots(VC)\,(\mathbf{16}) + e^- \rightarrow CH_3{}^{\bullet}CHCH_2(CO_3)^-\cdot\cdot Li^+\cdots(VC)\,(\mathbf{22}), \quad \text{(V)}$$

are 2.14, 2.74, 1.95, and 3.17 V, respectively, and they are rather close to the corresponding ones obtained from $Li^+(VC)-$CPCM (2.19 and 2.79 V)[34] and $Li^+(PC)_2-$CPCM (1.82 V). One recent cyclic voltammetry (CV) study indicates that the reduction potential (Au electrode, VC/THF/$LiClO_4$) of VC is 2.96 V and that of PC ranges from 2.56 to 3.16 V.[36] The theoretical reduction potentials based on the formation of ion-pair intermediates (**17** and **18** from reactions II and IV, respectively) qualitatively reproduce the experimental trend observed on a gold electrode surface, that indicates that VC has higher reduction potential, whereas those based on the anion radicals (**20** and **22** from reactions III and V) provide an opposite result. The reduction potential of VC (2.74 V) from reaction III is also numerically close to the CV measured value on the gold electrode (about 2.96 V) and that of PC (3.17 V) from reaction IV approaches its experimental upper limit. The present calculation for reduction potential neglects the effect of electrodes, which is being carried out using a finite cluster model for the Au surface and a H-truncated carbon cluster for the graphite electrode.

PC solvates Li^+ more strongly than VC, which is reflected by the shorter $O-Li^+$ distances in $(PC)Li^+(VC)$, 1.808 versus 1.826 Å, as shown in Figure 4, 1.88 versus 1.91 Å in **24** shown in Figure 5, as well as by the binding energies of Li^+ with the respective solvents (ZPE- and BSSE-corrected BE: 49.1 and 43.4 kcal/mol for PC and VC at B3PW91/6-311++G(d,p), see also Table 1). The application of the AIM method yields another indication for VCs weak solvation ability to Li^+: $\rho(r) = 0.041$ au, $\nabla^2\rho(r) = 0.360$ at the bcp between Li^+ and carbonyl oxygen of VC, and $\rho(r) = 0.043$ au, $\nabla^2\rho(r) = 0.379$ at the bcp between Li^+ and the carbonyl oxygen of PC. Considering the role that VC could play as an additive in PC or PC-based mixtures, these results imply that a strong solvation is not a critical factor for the efficiency of an additive. On the other hand, the VC-reduction intermediate (**17**) is more stable than the PC-reduction intermediate (**16**) by approximately 5 kcal/mol. Therefore, the reduction potential may be an important index for the efficiency of a lithium-ion battery electrolyte additive.

Because of the negligible effect of the VC molecule on the termination reactions of the radical anion caused by EC decomposition in $(EC)Li^+(VC)$,[34] only the termination reactions of the radical anion **20** are investigated, such as the further reduction path and the two favorable paths generating lithium alkyl dicarbonates. Generally, the ΔG of these reactions are extremely similar to the corresponding reactions in the case

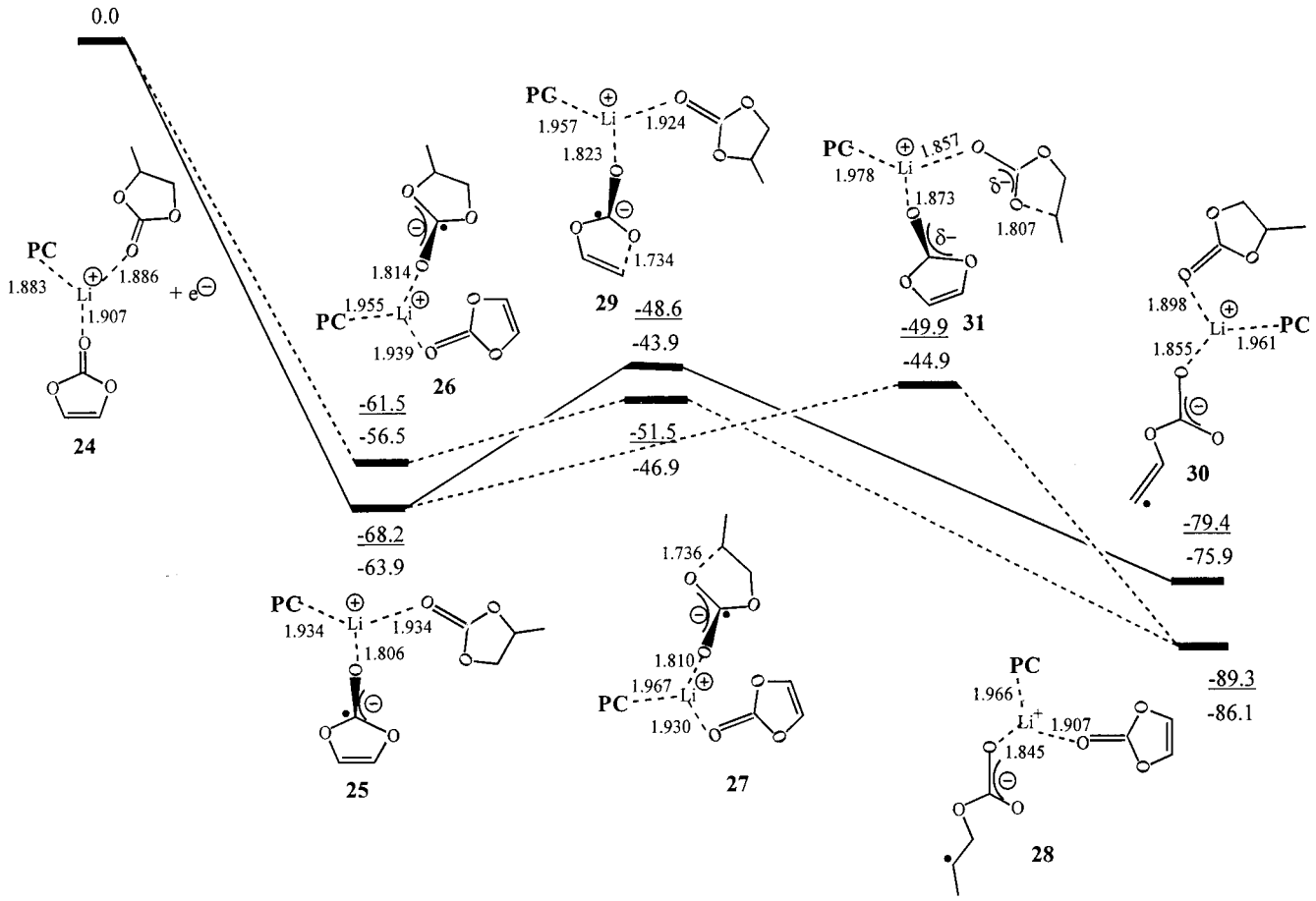

Figure 5. Potential energy (underlined data) and Gibbs free energy profile at 298.15 K for the reductive decomposition process of $(PC)_2Li^+(VC)$ with B3PW91/6-311++G(d,p)// B3PW91/6-31G(d) method.

TABLE 4: Relative Energies, Enthalpies, and Free Energies (in kcal/mol), Charge (*q*/e), Main Coefficients of Spin Densities (sd/e) for Stationary Points and Imaginary Frequency (ω/cm^{-1}) for Transition States in $(PC)Li^+(VC)$ and $(PC)_2Li^+(VC)$

						q[f]		sd[g]		
structures	ΔE^a	$\Delta E(0)^b$	$\Delta E_0{}^c$	$\Delta H(T)^d$	$\Delta G(T)^e$	Li	PC(VC)	C1	C2	w
$(PC)Li^+(VC)$										
16	0.0	0.0	0.0	0.0	0.0	+0.95				
17	**−71.3**	−73.5	−76.8	−76.9	−75.4	+0.75	(−0.81)	(0.65)		
18	**−67.7**	−69.5	−72.0	−72.3	−70.5	+0.78	−0.83	0.67		
19(TS,17↔20)	**−48.4**	−52.4	−56.7	−56.8	−55.2	+0.74	(−0.79)	(0.38)	(0.46)	−1008
20	**−82.7**	−85.7	−91.2	−91.2	−88.9	+0.74	(−0.81)		(1.1)	
21(TS,18↔22)	**−53.1**	−56.9	−60.5	−60.6	−60.0	+0.71	−0.78	0.44	0.40	−911
22	**−93.1**	−96.6	−101.4	−100.8	−101.6	+0.70	−0.78		1.0	
23(TS,17↔22)	**−53.0**	−57.3	−62.0	−61.8	−61.6	+0.69	−0.24	(0.44)	0.30	−740
							(−0.45)			
$(PC)_2Li^+(VC)$										
24	0.0	0.0	0.0	0.0	0.0	+0.98				
25	**−61.7**	−63.4	−68.2	−68.4	−63.9	+0.64	(−0.62)	(0.67)		
26	**−55.6**	−57.3	−61.5	−61.8	−56.5	+0.65	−0.70	0.68		
27(TS,26↔28)	**−42.4**	−46.0	−51.5	−51.8	−46.9	+0.68	−0.71	0.45	0.43	−890
28	**−79.7**	−83.1	−89.3	−88.8	−86.1	+0.72	−0.76		1.0	
29(TS,25↔30)	**−38.9**	−42.7	−48.6	−48.7	−43.9	+0.67	(−0.71)	(0.40)	(0.47)	−1023
30	**−70.0**	−72.8	−79.4	−79.1	−75.9	+0.73	(−0.81)		(1.0)	
31(TS,25↔28)	**−41.1**	−45.0	−49.9	−50.1	−44.9	+0.71	−0.35	(0.43)	0.38	−737
							(−0.39)			

[a] ΔE(B3PW91/6-31G(d)). [b] $\Delta E(0)$: ΔE(B3PW91/6-31G(d))+ ΔZPE(B3PW91/6-31G(d)). [c] ΔE_0: ΔE(B3PW91/6-311++G(d,p)//B3PW91/6-31G(d))+ ΔZPE(B3PW91/6-31G(d)). [d] ΔH: ΔE(B3PW91/6-311++G(d,p)//B3PW91/6-31G(d))+$\Delta\Delta H$(B3PW91/6-31G(d)). [e] ΔG: ΔE (B3PW91/6-311++G(d,p)//B3PW91/6-31G(d))+ $\Delta\Delta G$(B3PW91/6-31G(d). [f] CO_3 group belongs to the reactive PC or VC molecule, and the data in parentheses refer to the VC moiety. [g] C1 and C2 refer to carbonyl carbon and ethereal carbon, respectively, and the data in parentheses refer to the corresponding atoms of the VC moiety.

of $(EC)Li^+(VC)$. The ΔG of the further reduction to LiO_2-$COCH{=}CH^-$ is still a relatively small negative value, −29.0 kcal/mol. The direct dimerization path of the radical anion **20** resulting in lithium alkyl dicarbonate, $(CH{=}CHOCO_2Li)_2$ solvated by PC, exhibits also a very strong tendency to be formed reflected by a large negative ΔG of −105.2 kcal/mol.

The ΔG of the path forming another lithium alkyl dicarbonate, $LiO_2COCH{=}CHCHCH_3CH_2OCO_2Li$, with two tails solvated by PC and VC respectively, obtained through the cross dimerization of **20** with the radical anion **22,** is considerably more negative than that of path **A** in Figure 3 (−80.3 vs −59.2 kcal/mol), which reveals the crucial role of the unsaturated group in stabilizing these dicarbonates through electron delocalization. These two double-bond containing dicarbonates, together with lithium vinylene dicarbornate, $(CHOCO_2Li)_2$,[34] may further polymerize on the electrode surface, thus forming polyvinylene dicarbonate or oligomers with several repeated CH═CH units that considerably improve the passivation of graphite electrode in the presence of VC.

The reductive decompositions of **24** in Figure 5 are very similar to that of **16** from a mechanistic viewpoint. However, its adiabatic EA is decreased further (68.2 and 61.5 kcal/mol for VC- and PC-reduction in **24**) by the explicit inclusions of one more PC molecule, and the heats of formation for the radical anions are also decreased (−79.4 vs −91.2 kcal/mol for VC ring opening, −89.3 vs −101.4 kcal/mol for PC ring opening). The VC-reduction intermediate, **25,** gets extra stability from the additional PC molecule, for example, it has 6.7 kcal/mol lower energy than the PC-reduction intermediate, while only 4.8 kcal/mol in the case of $(PC)Li^+(VC)$. The EA corresponding to the PC reduction becomes nearly identical with that in the $Li^+(PC)_3$ cluster (61.5 vs 61.8 kcal/mol). The result is another strong indication that VC is more easily reduced than the PC molecule in the PC-based electrolyte of Li-ion batteries in which VC is used as an additive, and VC does not clearly improve the reduction capability of PC. Regarding the ring-opening reactions, similarly to the preceding results predicted by the CPCM approach for the cluster $(PC)Li^+(VC)$, the energy barrier for the PC-reduction intermediates, **26,** is decreased via the TS, **27**, as compared with that of **15** (10.0 vs 11.5 kcal/mol). For VC-reduction intermediates, the barrier for the VC-moiety via TS **29** remains close to that of **16** (19.6 vs 20.4 kcal/mol), whereas the inclusion of one more PC molecule considerably increases that of the PC-moiety via the TS **31** by 4 ∼ 5 kcal/mol (18.3 vs 14.8 kcal/mol).

On the basis of the above investigation, the additive role of VC on modifying the SEI film formation can be explained in two ways. First, since the VC molecule is more easily reduced than PC by approximately 0.2 V in the Li-salt/PC/VC electrolyte, it will be initially reduced to the more stable ion-pair intermediate, which may overcome a higher barrier of about 20 kcal/mol and may undergo a ring-opening decomposition with the help of the energy released by the formation of the intermediate, that is, **24** + $\mathbf{e}^-$ → **25** → TS, **29** → **30** as shown in Figure 5. VC has less chances to cointercalate into the graphite layers with the lithium ion because of its 5.0 kcal/mol lower ion−solvent binding energy than PC, hence its reduction may be mainly occurring at the edge of graphite electrode. The main products of the VC reductive decomposition are the lithium alkyl dicarbonates, $(CH{=}CHOCO_2Li)_2$, $LiO_2COCH{=}CHCHCH_3CH_2OCO_2Li$, and $(CHOCO_2Li)_2$, which are believed to be more proper passivating agents than those from PC reduction according to the sticky-finger model of adhesion to the graphite electrode.[33] Moreover, these compounds probably further polymerize because they contain double bonds and may form a highly cohesive and flexible surface film, which may be built up quickly preventing the destructive processes of the negatively charged graphite electrode in PC solutions. An alternative way to explain the role of VC, starting from the more stable VC ion-pair intermediate, consists on the homolytic ring opening taking place on the PC moiety instead of being on the reduced VC, via an intramolecular electron-transfer TS **31**, generating the more stable radical anion **28**, that is, **24** + $\mathbf{e}^-$ → **25** → TS, **31** → **28**. Thus, the cointercalation problem attributed to PC because of its weak reduction could be solved to some extent by the presence of VC. Actually, both proposed ways may contribute individually and in parallel manner to the role that VC plays as an additive.

Conclusions

High-level DFT-based calculations have been performed on the clusters $Li^+(PC)_n$ ($n = 2, 3$) and $(PC)_nLi^+(VC)$ ($n = 1, 2$)[37] to investigate the mechanism of the destructive behavior of PC that causes considerable irreversibility in lithium-ion batteries when PC alone is used as solvent and to elucidate the role of VC as an additive of the PC-based electrolyte. The main results and conclusions are summarized as follows: (1) The ΔG_r for the formation of the $Li^+(PC)_n$ clusters indicates that $Li^+(PC)_4$ is unlikely to exist and that the main components in lithium salt/PC lithium-ion battery electrolytes are $Li^+(PC)_2$ and $Li^+(PC)_3$, which is in good agreement with the recent ESI-MS investigation into the solvation of Li^+ in the lithium-ion electrolyte.[30] The clusters, $(PC)_nLi^+(VC)$ ($n = 1$ and 2), are mainly generated by the addition reactions between VC with $Li^+(PC)$ and $Li^+(PC)_2$, respectively, rather than by the substitution reactions between VC with $Li^+(PC)_2$ and $Li^+(PC)_3$. (2) The binding energies of carbonate solvents with lithium ion decrease in the order: PC > EC > VC (ZPE- and BSSE-corrected BE: 49.1, 47.4, and 43.4 kcal/mol at B3PW91/6-311++G(d,p) level), whereas their reduction potentials (RP) reverse, for example, RP estimated by the cluster-CPCM method for the ion-pair intermediate generations are 1.82 V for PC ($Li^+(PC)_2$, $\epsilon = 66.14$), 1.96 V for EC ($Li^+(EC)_2$, $\epsilon = 89.78$), and 2.03 V ($(PC)Li^+(VC)$, $\epsilon = 66.14$) or 2.08 V ($(EC)Li^+(VC)$, $\epsilon = 89.78$) for VC, respectively. These results imply that a strong solvation is not a critical factor for the efficiency of an additive, whereas the reduction potential may be an important index for selecting an additive of lithium-ion battery electrolyte. (3) Regarding the reductive decomposition, generally PC performs very similarly to EC in terms of reaction mechanisms. Although the generation path of the inorganic product, Li_2CO_3, becomes even less favorable than that in the case of EC it is difficult to ascribe the PC destructive behavior to this. It is possible that the mechanical stability of the film, such as the adhesion ability of the products, is another important reason, which is under investigation by MD and other techniques. (4) The addition of VC somewhat weakens the solvent cointercalation into graphite and stabilizes the reduction ion-pair intermediate because of its lower binding energy to lithium ion and higher reduction potential. Specifically, VC may play the role as an additive in PC-based solvent of lithium-ion batteries in the following manners: VC is initially reduced to a more stable ion-pair intermediate, which will undergo ring opening by a homolytic C (carbonyl carbon)−O rupture in two ways. One is that the reduced VC decomposes to form a radical anion via a barrier of about 20 kcal/mol and the subsequent radical anion termination would bring about proper products, such as lithium alkyl (CH═CH, CH═CH−CH═CH, CH═CH−$CHCH_3CH_2$, etc.) dicarbonate, a R−O−Li compound, and Li−C carbides, to build up an effective SEI film that would prevent further solvent reduction. These primary products mainly differ from those of PC in the double-bond CH═CH units. It is the double bond that may cause further polymerization of the primary species, forming polyvinylene dicarbonate or oligomers with several

repeated CH═CH units that considerably improve the passivation of graphite electrode in the presence of VC because of the formation of more cohesive and flexible films. Therefore, the role of VC in the PC-based electrolyte could be explained in terms of the simple surface reduction model developed by Aurbach et al.[4] On the other hand, because of approximately 6 kcal/mol lower ion−solvent binding energy of VC than PC, if it exists, the cointercalation of solvents into graphite layers at least is weakened so that the destruction of graphite because of the GIC is decreased to some extent. Starting from the VC-reduction intermediate, the ring opening occurs on the unreduced PC moiety rather than on the reduced VC, via an intramolecular electron-transfer TS, the energy barrier of which is about 3.0 kcal/mol lower than that of the former. In this way, both the solvent cointercalation and the lower reduction potential are improved. Therefore, the GIC model can also interpret the VC role in PC-based electrolyte solutions. Nevertheless, the stability difference between GIC from PC and PC/VC mixture needs further investigation. As described above, these positive factors such as preferred reduction, further polymerization of double-bond containing primary reduction products, and weak bonding to Li^+ may contribute not only individually but also in parallel manners to the role that VC plays as an additive.

Acknowledgment. This work was partially supported by NSF (Career Award Grant CTS-9876065 to P.B.B.), by Mitsubishi Chemical Corporation, and by DOE Cooperative Agreement DE-FC02-91ER75666. We acknowledge supercomputer resources provided by the National Computational Science Alliance under grants CHE000040N, CTS000016N, CTS00007N (Y.W., P.B.B.) and by NERSC.

References and Notes

(1) Armstrong, A. R.; Bruce, P. G. *Nature* **1996**, *381*, 499.
(2) Dominey, L. A. *Lithium Batteries. New Materials, Developments and Perspectives*; Elsevier: Amsterdam, 1994.
(3) Arora, P.; White, R. E.; Doyle, M. *J. Electrochem. Soc.* **1998**, *145*, 3647.
(4) Aurbach, D.; Levi, M. D.; Levi, E.; Schechter, A. *J. Phys. Chem. B* **1997**, *101*, 2195.
(5) Schechter, A.; Aurbach, D.; Cohen, H. *Langmuir* **1999**, *15*, 3334.
(6) Aurbach, D. *J. Power Sources* **2000**, *89*, 206.
(7) Wang, Y. X.; Nakamura, S.; Ue, M.; Balbuena, P. B. *J. Am. Chem. Soc.* **2001**, *123*, 11708.
(8) Besenhard, J. O.; Winter, M.; Yang, J.; Biberacher, W. *J. Power Sources* **1995**, *54*, 228.
(9) Bar-Tow, D.; Peled, E.; Burstein, L. *J. Electrochem. Soc.* **1999**, *146*, 824.
(10) Naji, A.; Ghanbaja, J.; Humbert, B.; Willmann, P.; Billaud, D. *J. Power Sources* **1996**, *63*, 33.
(11) Besenhard, J. O.; Fritz, H. P. *J. Electrochem. Soc.* **1974**, *3*, 329.
(12) Winter, M.; Besenhard, J. O. *Lithium Ion Batteries. Fundamentals and Performances*; Wakihara, M., Yamamoto, O., Eds.; Wiley-VCH: New York, 1999; p 127.
(13) Jeong, S.-K.; Inaba, M.; Abe, T.; Ogumi, Z. *J. Electrochem. Soc.* **2001**, *148*, A989.
(14) Peled, E. Lithium Stability and Film Formation in Organic and Inorganic Electrolyte for Lithium Battery Systems. In *Lithium Batteries*; Gabano, J. P., Ed.; Academic Press: New York, 1983.
(15) Peled, E.; Golodnitsky, D.; Menachem, C.; Bar-Tow, D. *J. Electrochem. Soc.* **1998**, *145*, 3482.
(16) Chung, G.-C.; Kim, H.-J.; Yu, S.-I.; Jun, S.-H.; Choi, J.-W.; Kim, M.-H. *J. Electrochem. Soc.* **2000**, *147*, 4391.
(17) Shu, Z. X.; McMillan, R. S.; Murray, J. J.; Davidson, I. J. *J. Electrochem. Soc.* **1995**, *142*, L161.
(18) Jehoulet, C.; Biensan, P.; Bodet, J. M.; Broussely, M.; Tessier-Lescourret, C. *Batteries for Portable Applications and Electric Vehicles*; The Electrochemical Society Proceedings Series: Pennington, NJ, 1997.
(19) Wrodnigg, G. H.; Besenhard, J. O.; Winter, M. *J. Electrochem. Soc.* **1999**, *146*, 470.
(20) Frisch, M. J.; Trucks, G. W.; Schlegel, H. B.; Scuseria, G. E.; Robb, M. A.; Cheeseman, J. R.; Zakrzewski, V. G.; Montgomery, J. A.; Stratmann, R. E.; Burant, J. C.; Dapprich, S.; Millam, J. M.; Daniels, A. D.; Kudin, K. N.; Strain, O. F. M. C.; Tomasi, J.; Barone, B.; Cossi, M.; Cammi, R.; Mennucci, B.; Pomelli, C.; Adamo, C.; Clifford, S.; Ochterski, J.; Petersson, G. A.; Ayala, P. Y.; Cui, Q.; Morokuma, K.; Malick, D. K.; Rabuck, A. D.; Raghavachari, K.; Foresman, J. B.; Ciolovski, J.; Ortiz, J. V.; Stefanov, V. V.; Liu, G.; Liashensko, A.; Piskorz, P.; Komaroni, I.; Gomperts, R.; Martin, R. L.; Fox, D. J.; Keith, T.; Al-Laham, M. A.; Peng, C. Y.; Nanayakkara, A.; Gonzalez, C.; Challacombe, M.; Gill, P. M. W.; Johnson, B.; Chen, W.; Wong, M. W.; Andres, J. L.; Head-Gordon, M.; Replogle, E. S.; Pople, J. A. GAUSSIAN 98, Revision A.9; Gaussian Inc.: Pittsburgh, PA, 1998.
(21) Becke, A. D. *J. Chem. Phys.* **1993**, *98*, 5648.
(22) Perdew, J. P. Unified theory of exchange and correlation beyond the local density approximation. In *Electronic Structure of Solids*; Ziesche, P., Eschrig, H., Eds.; Akademie Verlag: Berlin, 1991.
(23) Burke, K.; Perdew, J. P.; Wang, Y. *Electronic Density Functional Theory: Recent Progress and New Directions;* Plenum: New York, 1998.
(24) Perdew, J. P.; Burke, K.; Wang, Y. *Phys. Rev. B* **1996**, *54*, 16533.
(25) Breneman, C. M.; Wiberg, K. B. *J. Comput. Chem.* **1990**, *11*, 361.
(26) Barone, V.; Cossi, M. *J. Phys. Chem. A* **1998**, *102*, 1995.
(27) Cossi, M.; Barone, V.; Cammi, R.; Tomasi, J. *Chem. Phys. Lett.* **1996**, *255*, 327.
(28) Bader, R. F. W. *Atoms in molecules, a quantum theory*; Oxford Univ. Press: Oxford, UK, 1990.
(29) Klassen, B.; Aroca, R.; Nazri, M.; Nazri, G. A. *J. Phys. Chem. B* **1998**, *102*, 4795.
(30) Fukushima, T.; Matsuda, Y.; Hashimoto, H.; Arakawa, R. *Electrochem. Solid-State Lett.* **2001**, *4*, A127.
(31) Chung, G.-C.; Jun, S.-H.; Lee, K.-Y.; Kim, M.-H. *J. Electrochem. Soc.* **1999**, *146*, 1664.
(32) Aurbach, D.; Weissman, I.; Schechter, A.; Cohen, H. *Langmuir* **1996**, *12*, 3991.
(33) Ein-Eli, Y. *Electrochem. Solid-State Lett.* **1999**, *2*, 212.
(34) Wang, Y.; Nakamura, S.; Tasaki, K.; Balbuena, P. B. *J. Am. Chem. Soc.*, in press.
(35) Nakamura, S.; Ue, M. MCC, Japan. Private communication, 2000.
(36) Zhang, X. R.; Kostecki, R.; Richardson, T. J.; Pugh, J. K.; Ross, P. N. *J. Electrochem. Soc.* **2001**, *148*, A1341.
(37) Upon request, coordinates of the optimized structure will be provided. 2001.